Journal of Power Technologies 000 (0) (0000) 0–7

(????) Energy analysis and optimizing of hybrid WT/ PV cell in power systems

Name Surname *

Abstract

Due to the increasing need for energy and limited fossil resources on the one hand, and the increasing environmental pollution caused by the burning of these resources, on the other hand, the use of renewable energy has become more and more important. Wind and solar energy are one of the main types of renewable energy that has long attracted the human mind, so he has always thought about using these energies in the industry. In this study, the optimal combination of scattered production sources (wind-solar) has been added to a 33 IEEE bus system and beta distribution has been used to model wind speed. Also, load and production planning is 24 hours. The aim of this study is to improve voltage profiles, increase reliability and reduce losses. As a result, a 39% reduction in casualties in the presence of wind turbines and a 40% reduction in the presence of photovoltaic cells highlights the role of these resources in the grid.

Keywords: Modeling, fossil resources, renewable energy, losses.

1 Introduction

Due to the fact that distribution networks are the most suitable part for connecting to the power system, the most important step in using Distributed Generation (DG) is to place them in distribution networks and their optimal capacity. This is important because it reduces costs associated with casualties, reliability, and the cost of building production units[1]; [2]; [3]. and the posts are taken into account. On the other hand, uncertainty is one of the most important factors in increasing risk in the planning of power systems, so failure to consider this parameter leads to significant economic and technical losses.

Today, distributed generation sources are widely used in electrical systems due to their high importance in energy production[4]; [5]. Sincron generators are one of the most widely used types of dispersed products that are installed in medium pressure distribution systems. Because of the type of synchronous generator, DG performance capabilities, which have different operating modes such as power factor and voltage control, as well as the ability to install in different locations, can also affect the performance of voltage control and reactive power equipment[6]; [7]; [8]. Therefore, to ensure ULTC, especially DG, does not adjust the appropriate voltage in the system, the connection of the distribution system units must be done in coordination with other equipment of the system[9]; [10].

So far, several studies have been proposed on the control of voltage and reactive power in electrical energy distribution systems without examining the effect of DG. [11][12][13]; [11]; [12]; [14]; [15].Given the scope of the problem, most research has sought to achieve the best response in the shortest possible time, with only the feeder capacitors entering the optimal voltage and reactive power control, while the low capacitors not being considered [16]; [17]; [18].

In order to solve the multi-objective problem of voltage control and reactive power, the Phase building of target and constraint functions as well as metal hardening algorithm has been used to determine the final answer [19]; [20]. To reduce the search space, a time-based algorithm was used to predict the 24-hour forecast to determine the position of the pulse at any time interval, as well as the genetic algorithm to determine the optimal response[21] . The issue of voltage and reactive power control was performed in the presence of a scattering source of induction machine type (wind turbine) and using a combination of local and centralized control of equipment [21]; [22]. Feeder capacitors are controlled by a local voltage type controller: an abnormal position in the controller. However, Changer's low and high capacitors can be remotely controlled and thus controlled on a daily basis. Also, in both local and proposed controls, DG and the effect of how the change control function has been proposed have been investigated. Reactive voltage and power control is performed in the presence of scattered generator-based generator sources, and it is assumed that all equipment has only local control capability.

Meanwhile, assuming that the distribution system is equipped with automation, centralized control of con-

*Universiti ..., 00000 City, State if any, Country, e-mail

trol equipment is performed at any time of the day and night, observing the prevailing restrictions and with objectives such as: reducing losses and improving voltage profiles. This control is done in two modes with and without the presence of a scattered production source and in two modes of power factor control and voltage control. Also in the considered problem, DG is the effect of location and capacity. Due to the discrete space of the optimization problem, the genetic algorithm has been used to optimize and determine the position of the equipment 24 hours a day. At present, more than ever, the design and operation of power systems with maximum efficiency and maximum reliability and safety have been important, and this has been the motivation for a series of developments in transmission and distribution technology. One of these cases is reactive power control in transmission and distribution networks and today for various reasons such as increasing the transmission capacity of existing lines, preventing rapid and large changes in the voltage level, improving power factor, balancing the load and so on. It has become increasingly important.

2. Materials and methods

2.1 Network Modeling 33 Bus Considering Load Uncertainty and Production

In this section, we modeled the 33 bus network in a 24-hour, seasonal manner due to the uncertainty of load and production. The modeling of this section is based on the reference that we tested the model used in this reference on the 33 bus network. We modeled the 33-bus network with a new arrangement from the first research scenario. We compared the results for the voltage, loss, and network security profiles with the previous 33-bus distribution network layout to see the effect of the new layout on the network's basic parameters and in real time. Full information will be provided regarding the IEEE 33-standard standard network. The schematic of this network is shown in Figure 1.

As you can see from Figure (1), the 33-bus network consists of four main branches that are connected to the transmission network via a 1-bus and a transformer. Information about this network, including the maximum active and reactive power of the network, the resistance value and the reactance of the lines are given in Tables 1 and 2.

2.2 solar and wind

In the figure 2, can be seen see the hourly production of wind and solar. As can be seen, the figure on the right shows the wind and the left shows the sun. In addition to being hourly, the production rate is also shown seasonally. As mentioned earlier, the wind Weibull distribution is and the beta distribution is used to produce the sun.

Table 1: Maximum amount of active and reactive power of 33-bus network bus

Bus number	2	3	4	5	6
PL(KW)	100	90	120	60	60
qL(Kvar)	60	40	80	30	20
Bus number	7	8	9	10	11
PL(KW)	200	200	60	60	45
qL(Kvar)	10	10	20	20	30
Bus number	12	13	14	15	16
PL(KW)	60	60	120	60	60
qL(Kvar)	35	35	80	10	20
Bus number	17	18	19	20	21
PL(KW)	60	90	90	90	90
qL(Kvar)	20	40	40	40	40
Bus number	22	23	24	25	
PL(KW)	90	90	420	420	
qL(Kvar)	40	50	200	200	

2.3 Electrical load

The following figure shows the power consumption of the load per hour for different seasons. To show the uncertainty of the load, the load planning was considered as 24-hour and seasonal. So that we can bring the simulation results closer to reality with the possibility of load and production.

2.4 Possible power generation model

The production of wind and solar power is affected by weather conditions such as sunlight, wind speed and ambient temperature. Probability distribution functions (PDFs) can be used in a statistical manner to identify the random behavior of a renewable source (wind speed and solar radiation). The probability of solar radiation was considered following the Beta PDF. The beta distribution of solar radiation during the time segment t is as follows.[23].

$$\lambda = \frac{m_{actualair}}{m_{theoreticaair}} \quad (1)$$

$$f_s^t(s) = G(a^t+b^t)/(G(a^t)\cdot G(b^t))\cdot(s^t)^(a^t-1)\cdot(1-s^t)^(b^t-1) for a^t > 0; \quad (2)$$

$$f_s^t(s) = G(a^t + b^t)/(G(a^t).G(b^t)).(s^t)^(a^t - 1).(1 - s^t)^(b^t - 1)$$

$$for a^t > 0; b^t > 0 (1)$$

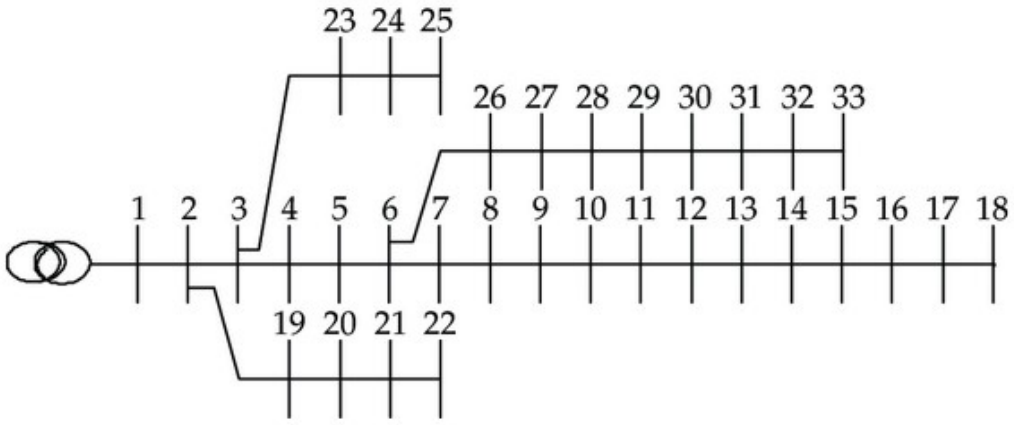

Figure 1: Schematic of IEEE 33 bus bar network

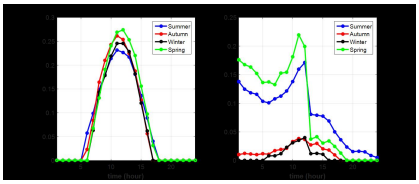

Figure 2: Wind and solar production per hour

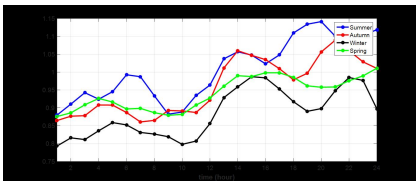

Figure 3: Power consumption per hour

Here B^t and a^t are Here are parameter forms in t, and Γ also indicates the gamma function.

The shape of the Beta PDF parameters can be calculated using the mean $(\mu_s^t)$and standard deviation (s_s^t) of radiation for the relevant time segment.

$$b^t = (1-\mu_s^t).((\mu_s^t(1+\mu_s^t))/(s_s^t)^2 - 1)(2)$$

$$a^t = (\mu_s^t * b^t)/((1-\mu_s^t))(3)$$

The decision to describe the random behavior of wind speeds is selected in a predetermined period of time Weibull PDF. The distribution of Weibull for wind speed $V^t(m/s)$ in the time interval tm can be expressed as follows [24-25]

$$f_v^t(v) = k^t/c^t.(v^t/c^t)^(k^t - 1).\exp(-(v^t/c^t)^(k^t - 1))forc^t > 1 : k^t > 0(4)$$

The parameter (k^t) and the scale factor(c^t) in the time segment tm are calculated as follows:

$$k^t = (s^t/(\mu_v^t))^(- 1.086)(5)$$

$$c^t = (\mu_v^t)/G(1+1/k^t)(6)$$

μ_v^t Ands_v^t are the mean standard wind deflection deviations in the time segment t. To calculate the output power of wind and solar DGs, continuous PDFs are divided into periods for a specific time frame. In each of them, solar radiation and wind speed are at a certain level. Production of PV and WT array power is controlled by the probability of all possible states for that time.

The average hourly output power of a PV array is related to a specific time segment. $t(P_p v^t)$ Which can be calculated as follows: [24]

$$P_P V^t = \sum_(g = 1)^(N_s)^- PG_P Vg * P_s(s_g^t)^\circ (7)$$

Here g determines the variable of state (period) and Ns the number of discrete states of solar radiation. Is also g a_{min} state / solar radiation level in t a_{min} time fragment. The probability of solar radiation for each state for each specific time frame is calculated as follows: [25]

$$P_s(s_g^t) = \int_0^(((s_g^t + s_(g+1)^t))/2)(f_s^t(s)dsforg = 1)$$

$$P_s(s_g^t) = \int_(((s_(g-1)^t + s_g^t))/2)^(((s_g^t + s_(g+1)^t))/2)^- f_s^t(s)dsforg = 2 \ldots (N_s - 1)^\circ (8)$$

$$P_s(s_g^t) = \int_(((v_(s-1)^t + v_s^t))/2)^[?]^- f_s^t(s)dsforg = N_s^\circ$$

Sunlight and the ambient temperature are the main factors influencing the output power of the Pv array. The power output of the Pv array in the average solar radiation (sag) for g a_{min} state / level is evaluated as follows [24].

Table 2: Resistance and reactance values of 33 bus bar network lines

Line number	1-2	2-3	3-4	4-5
rk	0.0922	0.4930	0.3660	0.3811
Xk	0.0470	0.2511	0.1846	0.1941
Line number	9-10	10-11	11-12	12-13
rk	1.04	0.19	0.37	1.46
Xk	0.74	0.06	0.12	1.15
Line number	17-18	2-19	19-20	20-21
rk	0.73	0.16	1.50	0.40
Xk	0.57	0.15	1.35	0.47
Line number	6-26	26-27	27-28	28-29
rk	0.20	0.28	1.05	0.80
Xk	0.10	0.14	0.93	0.70
Line number	5-6	6-7	7-8	8-9
rk	0.8190	0.1872	0.7114	1.0300
Xk	0.7070	0.6188	0.2351	0.7400
Line number	13-14	14-15	15-16	16-17
rk	0.54	0.59	0.74	1.28
Xk	0.71	0.52	0.54	1.72
Line number	21-22	3-23	23-24	24-25
rk	0.70	0.45	0.89	0.89
Xk	0.93	0.30	0.70	0.70
Line number	29-30	30-31	31-32	32-33
rk	0.50	0.97	0.31	0.34
Xk	0.25	0.96	0.36	0.53

$$PG_PVg(s_ag) = N_PVmod * FF * V_g * I_g(9)$$

Here N_{pvmod} is the sum of the number of Pv modules used for a Pv array. The current-voltage characteristic of the Pv module can be determined for a specific radiation level and ambient temperature T_A () using the following equations [24]; [25].

$$I_g = s_ag[I_SC + K_i(T_C - 25)](10)$$

$$V_g = V_OC - K_v * T_cg(11)$$

$$T_cg = T_A + s_ag((N_OT - 20)/0.8)(12)$$

$$FF = (V_MPP * I_MPP)/(V_OC * I_SC)(13)$$

T_cg The temperature of the solute in g Amin is the state of k_v and k_i, () is the coefficient of current and voltage temperature (A/ and V/), N_OT is the nominal operating temperature of the cell, FFt () is the filling factor, V_OC and I_SC are open circuit voltage (V) and The short circuit current (A) L_MPP and V_MPP are also the voltage (V) and current (A) at the maximum power point, respectively.

The average hourly output power of the WT is related to a specific time interval that can be calculated as follows:

$$P_WT^t = \sum_{(} g = 1)^{(}N_v)^{-}PG_WTg * P_v(v_g^t)^{\circ}(14)$$

WT power generation depends on its power performance curve. For nonlinear performance characteristics, the production of WT power at average wind speed for mode (g) is calculated as follows.

$$0v_ag < v_cinorv_ag > v_cout$$

$$PGwt = (a * v_ag^3 + b * P_rated)v_cin \leq v_ag \leq v_N$$

$$P_ratedv_N \leq v_ag \leq v_cout$$

Here P_{rated} is the maximum power that can be generated through WT. V_{cout} The wind speed is maximum. Fixes a and b are a function of the minimum wind speed V_{cin} and the nominal wind speed , which are calculated as follows:

$$a = P_rated/((v_N^3 - v_cin^3))(17)$$

$$b = (v_cin^3)/((v_N^3 - v_cin^3))(18)$$

Since DG distribution networks are active networks, the performance and control of the network is very interesting. Although there are a number of issues with the distribution network's performance, there are also major technical implications due to the influence of renewable DGs, such as network power loss, voltage stability, and network security discussed here.

Distribution networks are usually radially structured to reduce the complexity of protection. Assessing and reducing network power losses is essential to increase system efficiency. The average power loss per year can be calculated as follows:

Voltage stability indicators are used to assess the level of voltage stability of buses in the transmission or distribution network. These are very fast and effective tools for calculating the offline stability of voltages buses. The voltage stability index VSF (Voltage Stability Factor) for each bus -i + 1 in the time interval t can be expressed as follows.

$$VSF_(i+1)^t = (2V_(i+1)^t - V_i^t)(19)$$

The average annual voltage stability for the entire distribution network can be calculated an s follows:

$$VSF_a = (\sum_{(} t = 1)^{(} N_t) \sum_{(} i = 2)^{(} N_b) VSF_{(} i+1)^t)$$

$$/(N_t(N_b - 1)) \, (20)$$

N_b is the sum of the number of buses in the network. The bus -i + 1 is assumed to be in the main distribution post. The researchers looked at how high the VSF was. The network is more stable. If the line capacity increases from the existing transmission capacity, it will be overloaded, which is likely to cause network congestion, which in turn will cause various types of network disruptions. Line load (LL) is the load distribution (MVA) on the line according to the maximum power capacity (MVA) that is expressed for line i during the time interval "t" as follows:

$$LL_i^t = (L_{(} MVA.i)^t)/L_{(} MVA_m ax.i) \, (21)$$

Here $L_{MVAmax,i}$ and $L_{MVA,i}$ is the real capacity and maximum line i in t is the time interval. The annual average network security index (NSI) is plotted according to the loading of all lines in the network, which is as follows:

$$NSI_a = (\sum_{(} t = 1)^{(} N_t) \sum_{(} i = 1)^{(} N_l) LL_i^t)$$

$$/(N_t * N_l) \, (22)$$

Lower NSI values indicate a lower power risk than lines, which in turn increases network security. The proposed planning method should provide the equality and inequality constraints described below.

$$PGss - \sum_{(} i = 2)^N b^- Pd.i - Ploss = 0^\circ \, (23)$$

$$QG_s s - \sum_{(} i = 2)^N b^- Qd.i - Qloss = 0^\circ \, (24)$$

PG_{ss} and QG_{ss}The active and reactive power fed by mail in t is the timepiece. Lo Qloss. And Qloss the Ploss of active and reactive power in t is the time frame.

$$V_i^t \leq V_{(} \max .i)(25)$$

V^t_i And $V_{max.i}$ are the actual and maximum voltages in bus i for the time interval t.

Table 3: PV module specifications

Parameter	Amount
Voltage at the maximum point	28.36v
Flow at the maximum IMPP	7.76 A
Open circuit voltage Voc	36.96 V
Short circuit current	8.38 A
Nominal operating cell temperature	43 0c
Thermal flow	0.00545 A/0c
Thermal voltage	0.1278 V/0c

Table 4: Wind turbine specifications

Amount	Parameter	unit
Nominal output power	250	kw
Internal cutting speed	3	m/s
Nominal wind speed	12	m/s
External cutting speed	25	m/s

$$L_{(} MVA.i)^t \leq L_{(} MVA_{(} \max .i))(26)$$

$L_{MVA.i}$ And $L_{MVA.max}$ are the maximum and actual loads of line i in t of the time interval.

2.5 Photovoltaic cell and wind turbine

The renewable energy sources used in this system are photovoltaic cells and wind turbines. The specifications of wind turbine and photovoltaic cell can be seen in Tables 3 and 4.

As can be seen from Table 3, the maximum power output for a photovoltaic cell is 220 W. as can be seen table 4, the maximum power output of a wind turbine is 250 kW, this production capacity is possible for wind speeds of 12 m/s to more, the cutting speed for the turbine is 25 m/s.

3. Results

results with the presence of scattered production sources

Figure 4 shows the amount of electricity generated by wind turbines and photovoltaic cells regardless of the grid, also figure 5 also shows the amount of electricity generated by the wind turbine and the PV cell, taking into account the grid mentioned in the previous section.

According to Figure 4, in July, the amount of electrical energy produced by the PV cell is higher than that of the wind turbine, and in the other in the months, the production of the wind turbine is higher

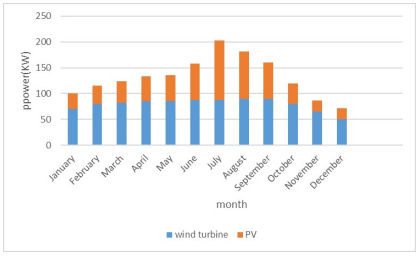

Figure 4: Wind turbine and PV generation without grid

than that of the cell. The highest and lowest electrical production of wind turbine is related to August and December months. For August electrical production is 90 KW/day and This amount for December is 50KW/day. The highest and lowest electrical production by PV cell is related to July and December months, which is to 118 and 22 KW/day, respectively.

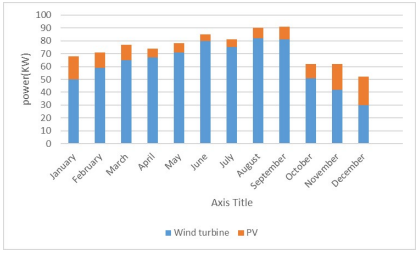

Figure 5: Wind turbine and PV generation with grid

As shown in Figure 5, the highest and lowest electrical production of renewable energy system is related to September and December months. For September electrical production is 91 KW/day and this amount for December is 50KW/day. For September, the amount of production by wind turbine and PV cell is 81 and 10KW/day, respectively. While for December, the amount of electricity produced by wind turbines and PV cell is 30 and 22KW/day, respectively.

The problem is solved as multi-objective, and the results show that the system parameters have been improved in multi-objective mode. The following tables show the parameters used for simulation.

In the table 5, can be seen the simulation results in the first scenario as a single goal and in the second scenario as a multi-objective. As can be seen, the voltage stability in both scenarios is almost equal, but the system security index and multi-objective loss improvements have improved compared to single-target mode.

Figure 6 shows the amount of electrical power generated by the wind turbine and the photovoltaic cell,

Table 5: Simulation results for Bus 33 system with security index and losses

	Security Index	losses
Primary system	0.59	0.89
WT	0.386	0.3929
PV	0.3772	0.4065
Optimal(1)	0.386	0.3922
Optimal(2)	0.3331	0.3388

Table 6: Simulation results for Bus 33 system with voltage profile and location of scattered products

	Voltage Profile	Location
Primary system	0.91	-
WT	0.9288	2 5 4 4
PV	0.9228	5 4 4 4
Optimal(1)	0.9288	27 17 13 11
Optimal(2)	0.919	17 9 8 7

taking into account the limitations, including optimization.

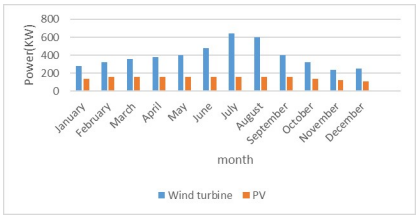

Figure 6: Optimal Wind turbine and PV generation with grid

According to Figure 6, the highest power generation by wind turbine is related to July with 640 kW/day, for this month, the amount of PV production is 160 KW/day. the lowest power generation by wind turbine is related to November with 240 kW/day, for this month, the amount of PV production is 120 KW/day. The highest and lowest power generation for renewable energy, consisting of wind turbines and photovoltaic cells, is in July and November. The total amount of electricity produced for the months of July and November is 800 and 360 kW/day, respectively.

4. Conclusion

Renewable energy sources have attracted a lot of attention due to their cleanliness and stability. Recently, a significant number of redistributed distributed products (DGs) have intermittent production patterns that are connected to the distribution network to meet the growing needs of the freight demand, making environmental threats ineffective. In-

tegrating the integration of renewable DGs into distribution networks is essential to ensure the quality and factor benefits of the network. In this paper, a simple and effective method for sizing, optimizing the placement of wind and solar DGs in distribution locations is presented, which also minimizes the loss of network power, improves voltage stability and network security. Accidental sunlight and wind speeds were also considered using possible appropriate models. Weighted particle optimization technique with weight accumulation has also been used to optimize target functions in which the bus voltage limit, line loading capacity, discrete size limit and DG penetration limits are considered.

References

1. (2017) Distributed generation deployment: State-of-the-art of distribution system planning in sustainable era. *Renewable and Sustainable Energy Reviews*, **77**.

2. (2019) Reliability/Security of Distribution System Network under Supporting by Distributed Generation. *Insight-Energy Science*, **2(1)**.

3.Alayi, R., Kasaeian, A., and Atabi, F. (2019) Thermal analysis of parabolic trough concentration photovoltaic/thermal system for using in buildings. *Environmental Progress & Sustainable Energy*, **38** (6), 13220.

4. (2020) Generation Management Analysis of a Stand-alone Photovoltaic System with Battery. *Renewable Energy Research and Application*, **1(2)**.

5.Tribioli, L., and Cozzolino, R. (2019) Techno-economic analysis of a stand-alone microgrid for a commercial building in eight different climate zones. *Energy Conversion and Management*, **179**, 58–71.

6.Cavalcanti, D., Perez-Ramirez, J., Rashid, M.M., Fang, J., Galeev, M., and Stanton, K.B. (2019) Extending Accurate Time Distribution and Timeliness Capabilities Over the Air to Enable Future Wireless Industrial Automation Systems. *Proceedings of the IEEE*, **107** (6), 1132–1152.

7.Nguyen, H.T., Battula, S., Takkala, R.R., Wang, Z., and Tesfatsion, L. (2019) An integrated transmission and distribution test system for evaluation of transactive energy designs. *Applied Energy*, **240**, 666–679.

8.Esmaeili, S., Anvari-Moghaddam, A., Jadid, S., and Guerrero, J.M. (2019) Optimal simultaneous day-ahead scheduling and hourly reconfiguration of distribution systems considering responsive loads. *International Journal of Electrical Power & Energy Systems*, **104**, 537–548.

9.Valverde, G., Shchetinin, D., and Hug-Glanzmann, G. (2019) Coordination of Distributed Reactive Power Sources for Voltage Support of Transmission Networks. *IEEE Transactions on Sustainable Energy*, **10** (3), 1544–1553.

10.Murty, V.V.V.S.N., and Sharma, A.K. (2018) Optimal coordinate control of OLTC DG D-STATCOM and reconfiguration in distribution system for voltage control and loss minimization. *International Transactions on Electrical Energy Systems*, **29** (3), e2752.

11.Kim, I., and Harley, R.G. (2020) Examination of the effect of the reactive power control of photovoltaic systems on electric power grids and the development of a voltage-regulation method that considers feeder impedance sensitivity. *Electric Power Systems Research*, **180**, 106130.

12.Ampofo, D.O., and Myrzik, J.M.A. (2019) A Comparative Study of Different Local Reactive Power Control Methods of Distributed Generation in Ghana. *2019 IEEE PES/IAS PowerAfrica*.

13.Eltamaly, A.M., Mohamed, Y.S., El-Sayed, A.-H.M., and Elghaffar, A.N.A. (2019) Analyzing of Wind Distributed Generation Configuration in Active Distribution Network. *2019 8th International Conference on Modeling Simulation and Applied Optimization (ICMSAO)*.

14.Liu, W., Chen, Y., Wang, L., Liu, N., Xu, H., and Liu, Z. (2020) An Integrated Planning Approach for Distributed Generation Interconnection in Cyber Physical Active Distribution Systems. *IEEE Transactions on Smart Grid*, **11** (1), 541–554.

15.Mahdad, B. (2019) Optimal reconfiguration and reactive power planning based fractal search algorithm: A case study of the Algerian distribution electrical system. *Engineering Science and Technology an International Journal*, **22** (1), 78–101.

16. (2019) Optimal capacitor placement in low voltage distribution grid.

17.Hao, Y., Yi, Y., Tang, J., and Shi, M. (2019) Active Reactive Power Control Strategy Based on Electrochemical Energy Storage Power Station. *2019 IEEE 3rd Conference on Energy Internet and Energy System Integration (EI2)*.

18.Chen, J., Xu, J., and Zhong, S. (2019) Optimal Voltage Control for Active Distribution Networks. *2019 IEEE Sustainable Power and Energy Conference (iSPEC)*.

19.Huang, Z., Fang, B., and Deng, J. (2020) Multi-objective optimization strategy for distribution network considering V2G-enabled electric vehicles in building integrated energy system. *Protection and Control of Modern Power Systems*, **5** (1).

20.Saffari, M., Kia, M., Vahidinasab, V., and Mehran, K. (2020) Integrated active/reactive power scheduling of interdependent microgrid and EV fleets based on stochastic multi-objective normalised normal constraint. *IET Generation Transmission & Distribution*, **14** (11), 2055–2064.

21.Alayi, R., Kasaeian, A., and Atabi, F. (2019) Optical modeling and optimization of parabolic trough concentration photovoltaic/thermal system. *Environmental Progress & Sustainable Energy*, **39** (2).

22.Shamel, A., Marefati, M., and Alayi, R. (2016) DESIGNING A PID CONTROLLER TO CONTROL A FUEL CELL VOLTAGE USING THE IMPERIALIST COMPETITIVE ALGORITHM. *Advances in Science and Technology Research Journal*, **10** (30), 176–181.

23.Sun, H., Guo, Q., Qi, J., Ajjarapu, V., Bravo, R., Chow, J., Li, Z., Moghe, R., Nasr-Azadani, E., Tamrakar, U., Taranto, G.N., Tonkoski, R., Valverde, G., Wu, Q., and Yang, G. (2019) Review of Challenges and Research Opportunities for Voltage Control in Smart Grids. *IEEE Transactions on Power Systems*, **34** (4), 2790–2801.

24. (2010) A novel power distribution strategy for parallel inverters in islanded mode microgrid.

25.Lappalainen, K., and Valkealahti, S. (2017) Output power variation of different PV array configurations during irradiance transitions caused by moving clouds. *Applied Energy*, **190**, 902–910.